Crustal Evolution of NW Iran: Cadomian Arcs, Archean Fragments and the Cenozoic Magmatic Flare-up

Article *in* Journal of Petrology · November 2017

DOI: 10.1093/petrology/egy005/4828038

10 authors, including:

Hadi Shafaii Moghadam
Karadeniz Technical University
117 PUBLICATIONS **2,854** CITATIONS

SEE PROFILE

William L. Griffin
Macquarie University
613 PUBLICATIONS **42,440** CITATIONS

SEE PROFILE

Xian-Hua Li
Chinese Academy of Sciences
441 PUBLICATIONS **30,600** CITATIONS

SEE PROFILE

José Francisco Santos
University of Aveiro
179 PUBLICATIONS **1,911** CITATIONS

SEE PROFILE

Earth and Planetary Science Letters 474 (2017) 83–96

Contents lists available at ScienceDirect

Earth and Planetary Science Letters

www.elsevier.com/locate/epsl

Neoproterozoic magmatic flare-up along the N. margin of Gondwana: The Taknar complex, NE Iran

Hadi Shafaii Moghadam [a,b,*], Xian-Hua Li [c], Jose F. Santos [d], Robert J. Stern [e], William L. Griffin [b], Ghasem Ghorbani [a], Nazila Sarebani [a]

[a] School of Earth Sciences, Damghan University, Damghan 36716-41167, Iran
[b] ARC Centre of Excellence for Core to Crust Fluid Systems and GEMOC ARC National Key Centre, Department of Earth and Planetary Sciences, Macquarie University, Sydney, NSW 2109, Australia
[c] State Key Laboratory of Lithospheric Evolution, Institute of Geology and Geophysics, Chinese Academy of Sciences, Beijing 100029, China
[d] Geobiotec, Departamento de Geociências, Universidade de Aveiro, 3810-193 Aveiro, Portugal
[e] Geosciences Dept., University of Texas at Dallas, Richardson, TX 75083-0688, USA

ARTICLE INFO

Article history:
Received 10 April 2017
Received in revised form 8 June 2017
Accepted 13 June 2017
Available online 4 July 2017
Editor: A. Yin

Keywords:
Cadomian magmatism
U–Pb zircon geochronology
magmatic flare-up
active continental magmatism
Gondwana

ABSTRACT

Magmatic "flare-ups" are common in continental arcs. The best-studied examples of such flare-ups are from Cretaceous and younger continental arcs, but a more ancient example is preserved in Late Ediacaran–Cambrian or Cadomian arcs that formed along the northern margin of Gondwana. In this paper, we report new trace-element, isotopic and geochronological data on ~550 Ma magmatic rocks from the Taknar complex, NE Iran, and use this information to better understand episodes of flare-up, crustal thickening and magmatic periodicity in the Cadomian arcs of Iran and Anatolia. Igneous rocks in the Taknar complex include gabbros, diorites, and granitoids, which grade upward into a sequence of metamorphosed volcano-sedimentary rocks with interlayered rhyolites. Granodioritic dikes crosscut the Taknar gabbros and diorites. Gabbros are the oldest units and have zircon U–Pb ages of *ca* 556 Ma. Granites are younger and have U–Pb zircon ages of *ca* 552–547 Ma. Rhyolites are coeval with the granites, with U–Pb zircon ages of ~551 Ma. Granodioritic dikes show two U–Pb zircon ages; *ca* 531 and 548 Ma. Geochemically, the Taknar igneous rocks have calc-alkaline signatures typical of continental arcs. Whole-rock Nd and zircon O–Hf isotopic data show that from Taknar igneous rocks were generated via mixing of juvenile magmas with older continental crust components at an active continental margin. Compiled geochronological and geochemical data from Iran and Anatolia allow identification of a Cadomian flare-up along northern Gondwana. The compiled U–Pb results from both magmatic and detrital zircons indicate the flare-up started ~572 Ma and ended ~528 Ma. The Cadomian flare-up was linked to strong crustal extension above a S-dipping subduction zone beneath northern Gondwana. The Iran–Anatolian Cadomian arc represents a site of crustal differentiation and stratification and involved older (Archean?) continental lower–middle crust, which has yet to be identified *in situ*, to form the continental nuclei of Anatolia and Iran. The Cadomian crust of Anatolia and Iran formed a single block "Cimmeria" that rifted away from northern Gondwana and was accreted to southern Eurasia in late Paleozoic time.

1. Introduction

Magmatism in continental arcs is often episodic, with high-volume magmatic flare-ups separated by lulls (Ducea and Barton, 2007; Paterson and Ducea, 2015). Magmatic arcs commonly flare up every 30–70 Ma, due either to tectonic changes such as rapid slab retreat, change in dip angle or slab break-off, or to thermal runaway due to pooling of mafic magmas in the lower crust (Ducea et al., 2010). Such flare-ups are characterized by felsic magmas; significant crustal inputs are indicated by high bulk-rock $^{87}Sr/^{86}Sr$ and low εNd, and high $\delta^{18}O$ and low εHf in zircon (Ducea and Barton, 2007).

Ideas about magmatic flare-ups and their causes were developed for Cretaceous and younger continental arcs, where the igneous rocks are best exposed and include the volcanic cover associated with plutons (*e.g.*, see Ducea and Barton, 2007). These ideas also provide a new way to think about ancient continental arcs,

* Corresponding author at: ARC Centre of Excellence for Core to Crust Fluid Systems and GEMOC ARC National Key Centre, Department of Earth and Planetary Sciences, Macquarie University, Sydney, NSW 2109, Australia.
E-mail address: hadishafaii@yahoo.com (H.S. Moghadam).

http://dx.doi.org/10.1016/j.epsl.2017.06.028
0012-821X/

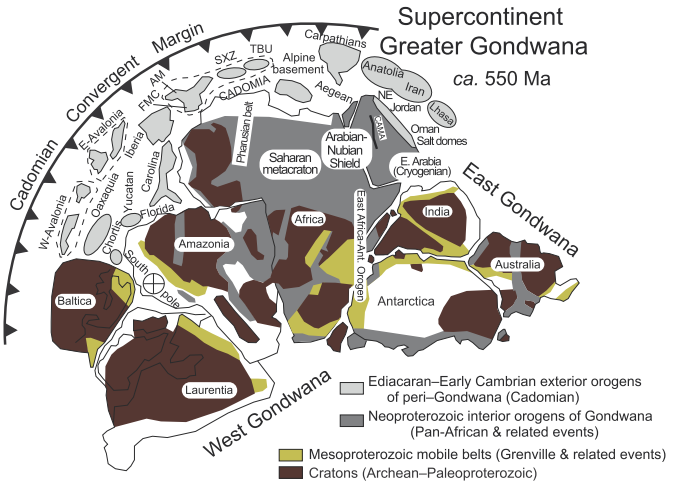

Fig. 1. Paleogeography of the Cadomian–Avalonian active margin and related major peri-Gondwanan terranes at ~550 Ma (modified after Linnemann et al., 2010). AM Armorican Massif, FMC French Massif Central, SXZ Saxo-Thuringian Zone (part of the Bohemian Massif), TBU Teplá-Barrandian Unit (part of the Bohemian Massif). Location of the Central Arabian Magnetic Anomaly (CAMA) separating Cryogenian–Ediacaran crust of the Arabian–Nubian Shield from Cryogenian crust of E. Arabia is from Stern and Johnson (2010). It is not surprising that northern Arabia hosts a tract of Cadomian crust, as Arabia projects farther north than other Gondwana margins. Distribution of Cadomian igneous rocks in NE Arabia is after Stern et al. (2016) and Thomas et al. (2015).

most of which are deeply eroded, buried by younger sediments, and disrupted by faulting.

Increasing evidence shows that a vigorous continental arc existed on the northern margin of the Greater Gondwana supercontinent during Late Ediacaran–Early Paleozoic time (600–500 Ma) (Fig. 1). This is referred to as the Cadomian, although some segments, especially in the west, are called Avalonia. Although both Cadomia and Avalonia formed along the Neoproterozoic active margin of Gondwana, these have different Paleozoic histories (*e.g.*, Nance et al., 2010).

This huge arc system needs further study, using outcrops that now are scattered across southern Europe, SW Asia, and perhaps into Central Asia and China. Unraveling the nature of this ancient and eroded continental arc from geochronologic, geochemical, and tectonic perspectives has great significance for understanding the formation and evolution of Cadomian continental crust including a magmatic flare-up.

Here we present new zircon U–Pb–Hf–O data and whole-rock Sr–Nd isotopic data for the Taknar complex of NE Iran, a typical example of a Cadomian granitic–gabbroic–rhyolitic suite. This is an excellent example to study because it contains both plutonic and volcanic rocks. The new data from Taknar, and from other Iranian Cadomian outcrops, are used to constrain the Ediacaran–Early Cambrian paleogeography and geodynamic setting of continental crust that now underlies the Iranian–Turkish plateau. We compare the Cadomian of Iran with that of Anatolia and evaluate the suitability of the magmatic flare-up model for understanding the Cadomian crust of this region and the thermal state of the upper mantle and lower crust of Greater Gondwana during that time.

2. Geological framework

2.1. The Cadomian orogen and arc

The Cadomian orogen reflects a Late Ediacaran to Early Cambrian peripheral accretionary margin and magmatic arc above a S-dipping subduction zone (subduction of Prototethys oceanic lithosphere) beneath northern Gondwana (Fig. 1; Linnemann et al., 2010; Moghadam et al., 2015a, 2015b).

Cadomian magmatic activity was diachronous and a transtensional setting as indicated by local volcano-sedimentary basins. In the eastern part of the arc in Iran and Turkey, subduction-related magmatism occurred 620 to 540 Ma, followed by the intrusion of younger arc-related granitoids from 540 to 520 Ma, which reflects crustal heating, perhaps related to slab break-off (Linnemann et al., 2010).

As a result of extension above the Cadomian subduction zone, one or more back-arc basins opened between the Cadomian arc and Greater Gondwana during latest Ediacaran and Early Cambrian time (Abbo et al., 2015; Linnemann et al., 2008). These basins continued opening to form the Rheic Ocean beginning at ~530 Ma, allowing Cadomian arc fragments to migrate north. Younger (<530 Ma) Cadomian ophiolites may be remnants of these marginal basins (von Raumer et al., 2015), but older (>540 Ma) ophiolites probably are related to initiation of the Cadomian subduction zone. Thus, the older ophiolites may indicate a trace of Prototethys forearc lithosphere, a Neoproterozoic Ocean between Laurasia in the north and Gondwana in the south. Paleotethys Ocean was different from Prototethys and refers to Paleozoic oceanic remnants between Greater Gondwana and a series of Gondwana-derived continental blocks such as Turan and/or Lhasa blocks (*e.g.*, Stampfli et al., 1991). The trace of Paleotethys Ocean with a 380–382 Ma old crustal section is now recognized in NE Iran (Moghadam et al., 2015a, 2015b). Cadomian and Avalonian fragments now form basement within the Paleozoic orogenic belts of eastern North America, Europe, Turkey, and Iran. As the Rheic Ocean widened, the rifted margin of Gondwana evolved to a passive margin and accumulated thousands of meters of clastic sediments (Linnemann et al., 2008). Cadomian arc rocks – mostly felsic intrusives – and associated sediments are documented many places in the basement of Europe, SW of the boundary between the Baltic craton and Cadomian accreted terranes (Trans-European Suture or Sorgenfrei–Tornquist–Teisseyre Zone) such as Iberia, Armorica and Bohemia (Linnemann et al., 2011; Nawrocki and Poprawa, 2006; Balintoni et al., 2010). It is not known why arc magmatism stopped at ~500 Ma, well before these terranes collided with the southern margin of Laurasia in Late Paleozoic time.

Number of studies have focused on various aspects of Cadomian sequences, including igneous geochemistry, and metamorphic and sedimentary provenance analysis (*e.g.*, Linnemann et al., 2007a, 2007b; Nance et al., 2010; Balintoni et al., 2010; Pereira et al., 2012; Murphy et al., 2013; Orejana et al., 2015), the general picture remains fragmentary, due to the scarcity of precise radiometric ages and geochemical and isotopic data. We are particularly interested in improving our understanding of the Cadomian basement of Iran and Turkey (Fig. 2).

Cadomian igneous rocks in NE Iran are known from regions such as Torud, Taknar and southeast of the Taknar complex (Fig. 2). There are some U–Pb dating as well as isotopic data on basement rocks near Torud (Fig. 2; Moghadam et al., 2015a, 2015b). Here, we describe three groups of igneous rocks that are exposed in the Taknar region (Fig. 2) and provide new zircon U–Pb–Hf–O and bulk rock Sr–Nd isotopic data. We use these data to explore the age and nature of the Cadomian high-flux magmatism in Iran.

2.2. Geology of the Taknar complex

The Taknar complex lies along the northern edge of the Lut Block within the Kashmar–Kerman Tectonic Zone, a nearly 600 km-long, arcuate and structurally complex fault-bounded belt that separates the Tabas and Yazd blocks of NE Iran (Fig. 2). This zone exposes deep sections of the central Iranian basement. The Taknar complex is a $\sim 10 \times 30$ km^2 tectonic slice between the Late Cretaceous Sabzevar ophiolite to the NNW and Cenozoic magmatic rocks to the east and west (Fig. 3a). The complex is bordered by

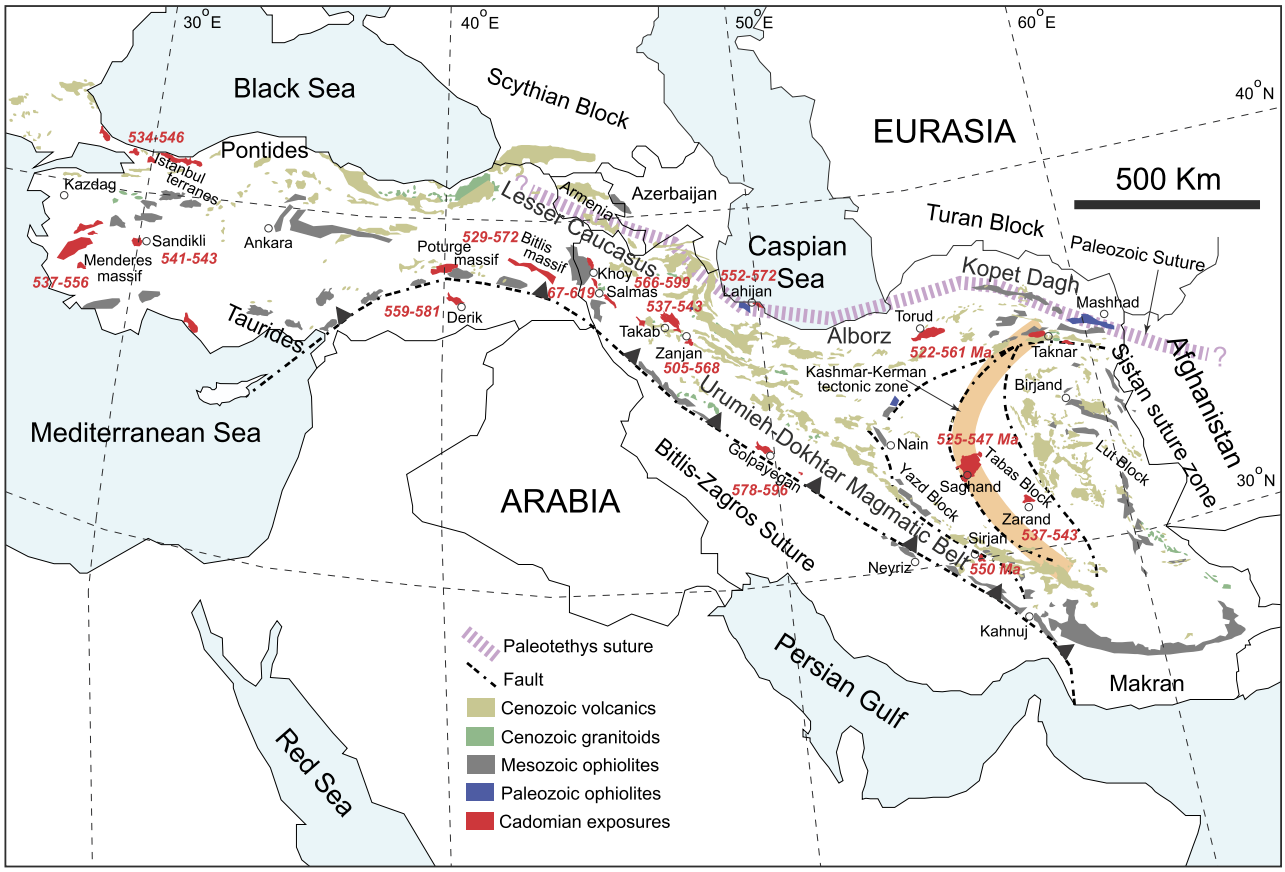

Fig. 2. Simplified geological map of Iran–Turkey showing the distribution of Cenozoic igneous rocks, Paleozoic–Mesozoic ophiolites and the Cadomian basement rocks.

the Dorouneh fault and Quaternary alluvium to the south and by the Taknar reverse fault to the north (Fig. 3b). Previous data from the Taknar complex (Bagherzadeh et al., 2015) include U–Pb zircon ages on two rock units with limited constraints on the nature of the Cadomian orogen in Iran.

Three Cadomian magmatic rocks can be distinguished in the Taknar complex, from oldest to youngest, these are: intermediate to mafic intrusive rocks; rhyolitic lavas and tuffs, and Bornavard granitoids (Fig. 3b). These are described further below.

2.2.1. Taknar rhyolites

Taknar Formation (or Taknar rhyolites) consists of three volcano-sedimentary sequences (including felsic lavas and green acidic tuffs, minor intercalated sandstones and siltstones, and slightly metamorphosed pelitic slates and phyllites) that may be equivalent to the rhyolites of the Kahar and Qara–Dash Formations in N–NW Iran and the Derik volcanics and associated volcaniclastic sediments in southeast Anatolia (Gursu et al., 2015). These rhyolites probably are the older equivalents of the Zarand rhyolites in south central Iran, which yield zircon U–Pb ages of *ca* 543–537 Ma (Fig. 2). The Taknar Formation has been subdivided into three members (Muller and Walter, 1983). The lower member consists of approximately 120 m of greenish tuffs, rhyolites and ignimbrites. The middle member, ~150–350 m thick, comprises minor carbonates, slightly metamorphosed siltstone, sandstone, greywacke, tuff and rhyolite, showing that this stage of the Cadomian arc formed near sea level. The upper member is composed of phyllite and slate, with rhyolites occurring as thin (~1 m) to thick layers (~ >10 m), unconformably overlain by thin phyllites (Fig. 3c). Deformed rhyolites with mylonitic structures and stretching lineation occur locally. These deformed rhyolites also contain quartz porphyries and elongated amphibole clots.

2.2.2. Cadomian mafic-intermediate intrusive rocks

Gabbros and diorites are common around the village of Kasf (Fig. 3b). These intrusions are intruded by abundant leucocratic granitic, granodioritic to leuco-gabbroic dikes, and pegmatitic, amphibole-rich dikes. The contacts between the Bornavard granites and mafic-intermediate intrusions are in most cases faulted, but some intrusive contacts show that gabbroic–dioritic rocks are older than Bornavard granitic rocks. No intrusive contact of Taknar rhyolites or tuffs with mafic-intermediate intrusive rocks has been found (Fig. 3c).

2.2.3. Bornavard granitoids

These granitoids comprise granites, leucogranites, monzogranites, granodiorites and tonalites with U–Pb zircon ages of 540–550 Ma and $\varepsilon Nd(t) = +2.5$ to -6.7, indicating the involvement of older crust (Bagherzadeh et al., 2015). Rare diabasic dikes (av. 1 m thick) intrude the granitoids and gabbroic–dioritic enclaves are common. The Bornavard granites may intrude the Taknar Formation (Bagherzadeh et al., 2015; Muller and Walter, 1983), but no high-*T* metamorphic haloes have been found. Locally granitoids show intrusive contacts with green tuffs. The Bornavard granites are unmetamorphosed, but locally cataclasized along shear zones.

Field observations (and zircon U–Pb ages, see next section) show that the Taknar complex mafic-intermediate intrusions are the oldest rocks and crosscut by younger granitoid dikes and also by Bornavard granites. The sequence is covered by Taknar Formation volcano-sediments. Bornavard granites were injected into the Taknar Formation volcano-sediments.

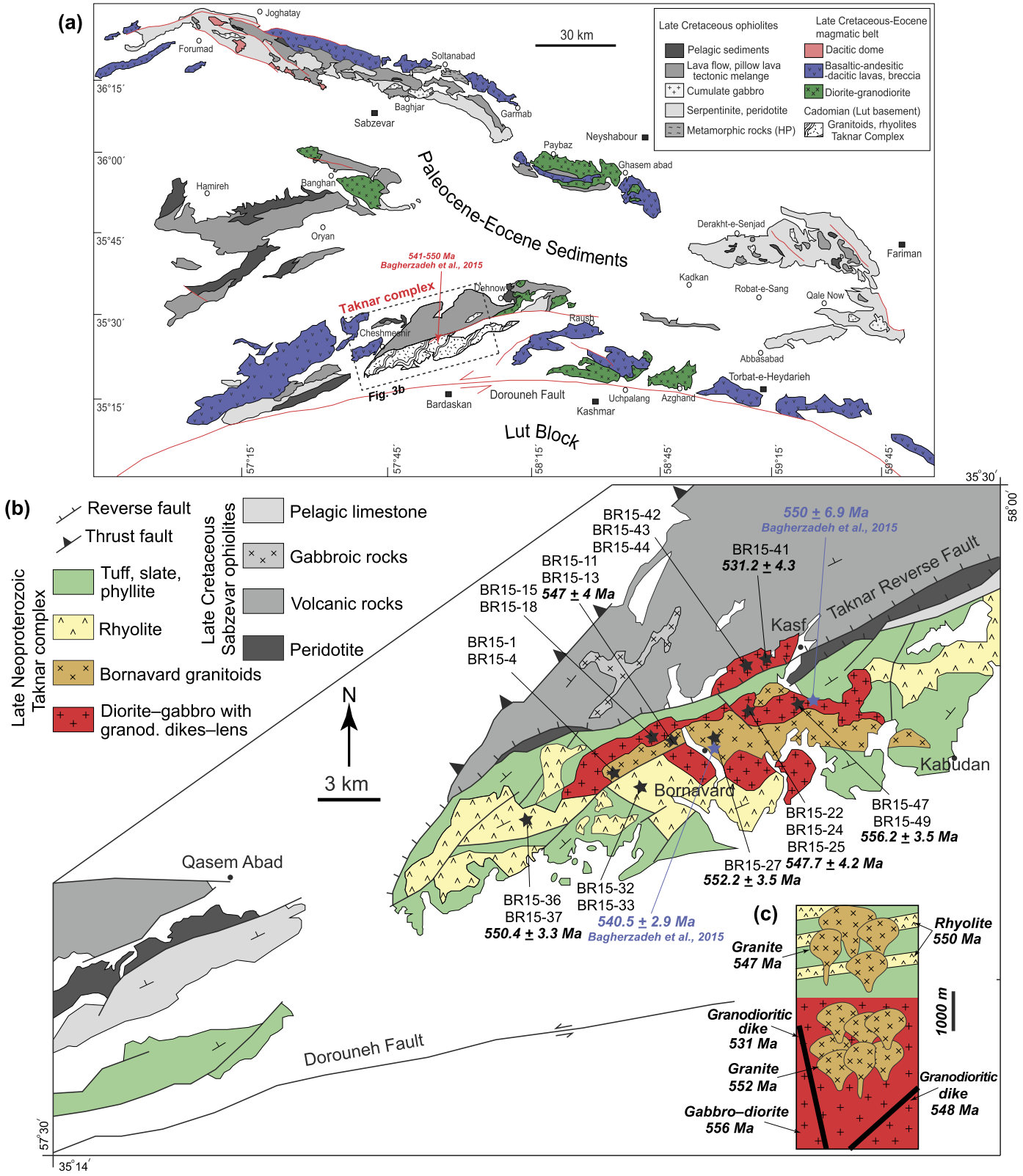

Fig. 3. (a) Geological map of the Sabzevar–Fariman region, north of the Dorouneh Fault, with emphasis on the distribution of ophiolitic, arc-related Late Cretaceous–Eocene rocks and Cadomian exposures. (b) Simplified geological map of the Taknar complex showing sample localities and available U–Pb age data (modified after Kashmar 1/250000 map, Geological Survey of Iran). U–Pb data from Bagherzadeh et al. (2015) is also shown for comparison. (c) Schematic lithological column showing the relationships between rocks units in the target areas and zircon U–Pb ages obtained during this study.

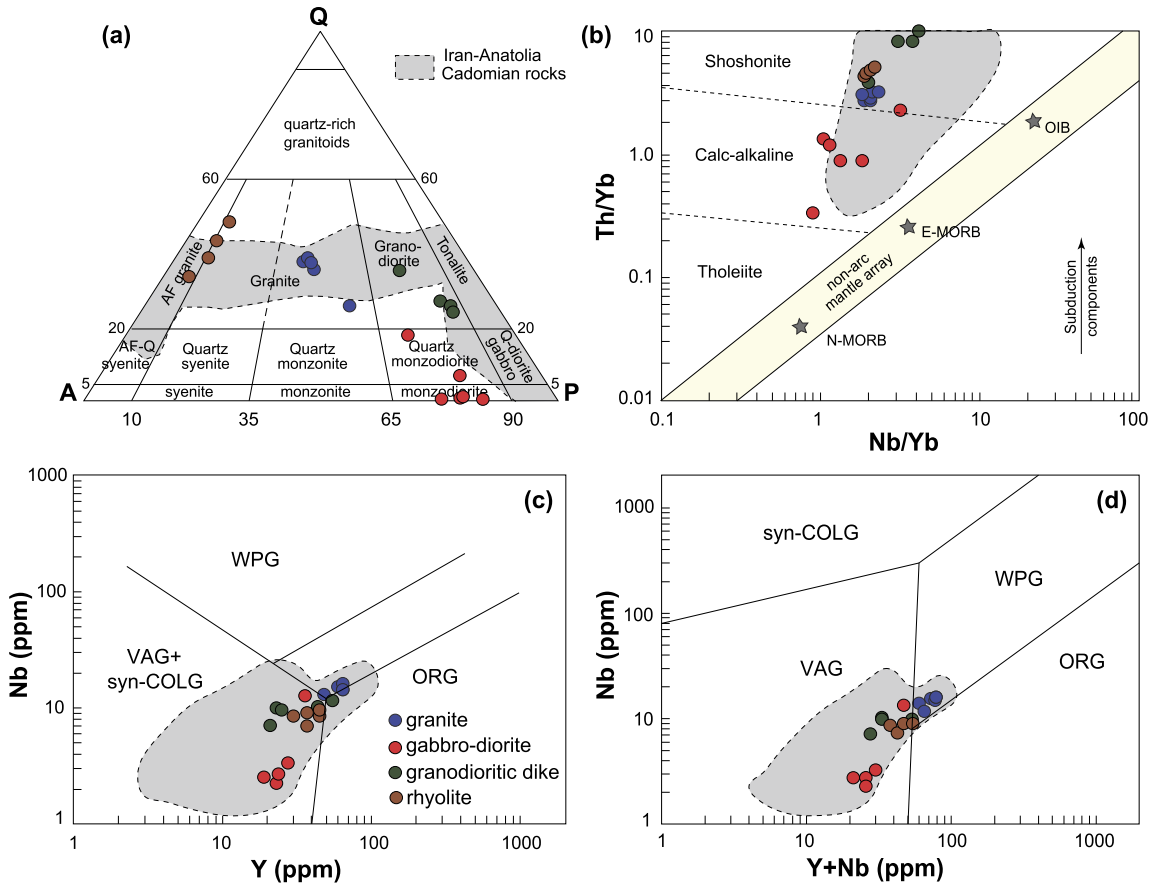

Fig. 4. (a) Quartz–Alkali feldspar–Plagioclase (QAP) normative classification diagram (Streckeisen, 1979) for Taknar Cadomian rocks. (b) Th/Yb *vs* Nb/Yb (Leat et al., 2004), (c) Nb *vs* Y and (d) Nb *vs* Y + Nb diagrams (Pearce et al., 1984) for Taknar Cadomian rocks. Data for Iran Cadomian rocks are from Moghadam et al. (unpublished data) except those for Torud data, which are from Moghadam et al. (2015a, 2015b). (AF granites = alkali feldspar granites, OIB = Oceanic Island Basalts; WPG = Within Plate Granites; VAG = Volcanic Arc Granites; ORG = Oceanic Ridge Granites; syn-COLG = syn-Collisional Granites).

3. Analytical procedures

We have used six main analytical procedures including: 1) X-Ray Fluorescence (XRF) and Inductively Coupled Plasma–Mass Spectrometry (ICP-MS) for whole-rock major- and trace-element analyses; 2) Cathodoluminescence imaging of zircons; 3) Secondary ion mass spectrometry (SIMS) for U–Pb zircon dating and O-isotope compositions; 4) Multi-Collector Inductively Coupled Plasma–Mass Spectrometry (MC-ICP-MS) to analyze zircon Lu–Hf isotopes; and 5) Thermal ionization mass spectrometry for of Sr and Nd isotopes in whole-rock samples. We studied ~50 samples petrographically, 20 for whole-rock chemical analysis (6 granitoid, 4 gabbro, 2 diorite, 4 granodioritic dike and 4 rhyolitic lava), 6 for SIMS U–Pb zircon ages and O isotopes, 6 for Lu–Hf analysis and 15 for Sr–Nd isotopes. We have selected fresh samples for whole rock geochemistry. Least-altered samples with different whole rock Rb/Sr and Sm/Nd ratios were selected for Sr–Nd isotope geochemistry. Our strategy for SIMS U–Pb dating (and zircon Hf–O) was to analyze representatives of the different rock types (gabbro, granite, dikes, and rhyolite). We sampled from different geographic locations to cover all rocks units from nearly all parts of the studied area. Analytical details are presented in Appendix A. A compilation of our data and all published geochronological-geochemical data is presented in Supplementary Table 1. Analytical procedures for our unpublished data for other Cadomian rocks of Iran are presented in Appendix B.

4. Results

4.1. Sample description and petrography

Location of the studied samples within the Taknar complex and their relations are presented in Fig. 3b and c. Felsic volcanic rocks of the Taknar complex are aphyric to porphyritic with quartz, sanidine and rare plagioclase phenocrysts in a groundmass of microcrystalline quartz and intergrowths of albitic plagioclase and potash feldspars. Tiny crystals of magnetite and apatite are common. Amphibole is rare, but when present usually occurs as elongated clots of magnesio-hornblende. Some rocks show traces of mylonitization. Felsic volcanic rocks are unmetamorphosed, but the groundmass and feldspar phenocrysts are replaced by sericite, clay minerals, calcite and titanite. Acidic tuffs and phyllites are very fine-grained, and acidic tuffs are rich in chlorite.

In the QAP (quartz–alkali feldspar–plagioclase) diagram (Streckeisen, 1979) the felsic volcanics plot in the field of rhyolite, while granitoids are granite and granodiorite. Granites are coarse-grained and contain quartz (35–37 vol.%), orthoclase (24–26%) and plagioclase (34–38%). Quartz (av. 3–4 mm) shows slightly undulose extinction. Plagioclase is mostly unzoned and slightly altered into sericite and clay minerals. Mafic minerals are rare, but occasionally chloritized amphibole is present. Apatite and magnetite are accessory minerals. Granodiorites contain coarse-grained plagioclase (~48%) and amphibole (4–5%) and fine-grained (1–2 mm) quartz (23%).

Gabbroids are subdivided into monzodiorite and monzogabbro to quartz-bearing monzodiorite (Fig. 4a). They rarely contain quartz

(except in monzodiorite), but variable modal plagioclase (50–70%) and alkali feldspar (5–15%). Plagioclase and alkali feldspar show variable alteration into clay minerals, sericite, epidote and titanite. Amphibole in dioritic rocks (20–30%) is altered into chlorite. Clinopyroxene is the main component of the gabbros and shows intense alteration into chlorite and actinolite. Traces of altered olivine are present, and accessory ilmenite and magnetite. Granodioritic dikes intruding the gabbroids contain quartz (25–30%), plagioclase (60–70%) and orthoclase (<10%) (Fig. 4a) and minor amphibole and apatite.

4.2. Zircon U–Pb dating

Fig. 5 shows the U–Pb zircon ages obtained in this study for two Bornavard granites, one gabbro, two tonalitic dikes intruding the intermediate-mafic rocks, and one Taknar dacite. We selected these rocks based on rock diversity and geographic locations to cover all rocks units from nearly all parts of the studied area. U–Pb geochronology results are provided below.

4.2.1. Sample BR15-37

This is a porphyritic, mylonitic rhyolite with quartz and sanidine phenocrysts. CL images of zircons revealed neither inherited cores nor metamorphic rims. Zircons are ~50–70 μm long. Most have oscillatory zoning and some show evidence of melt-zircon interaction. They contain 276–1394 ppm U, 124–715 ppm Th and Th/U = 0.3–1.4. We analyzed 20 zircon grains from this sample (Supplementary Document 3). The common-lead content is low, with $f_{206} = 0.03$–0.22%. Nineteen analyses (Fig. 5) yield a concordia age of 550.5 ± 3.3 Ma (MSWD = 0.05); this is taken as the crystallization age of the rhyolitic lavas.

4.2.2. Sample BR15-49

This is a medium-grained gabbro with amphibole, plagioclase and pyroxene. Zircons are large (>100 μm) and euhedral and most show oscillatory zoning. They contain 124–1326 ppm U, 51–972 ppm Th contents and Th/U from 0.4–1.3 (Supplementary Document 3). The common-lead content is low, with $f_{206} = 0.01$–0.44%. Out of twenty-four analyses, eighteen yield a concordia age of 556.2 ± 3.5 Ma (MSWD = 0.07; Fig. 5). This is taken as the crystallization age of the gabbros. Five other analyses show $^{206}Pb/^{238}U$ ages of *ca* 569 to 585 Ma and may represent inherited zircons.

4.2.3. Sample BR15-24

This is a coarse-grained granodioritic dike intruding the gabbroic rocks. Zircons are large (>100 μm) and euhedral; most have unzoned cores and zoned rims. They have 109–633 ppm U, 77–519 ppm Th and Th/U from 0.3–0.9 (Supplementary Document 3). The common-lead content is low, with $f_{206} = 0.04$–0.74%. Out of twenty analyses, thirteen define a concordia age of 547.7 ± 4.2 Ma (MSWD = 1.2; Fig. 5). The other analyses (magmatic cores) are slightly older, but are concordant and show a concordia age of 565.6 ± 5.9 Ma (not shown).

4.2.4. Sample BR15-41

This is a fine-grained granodiorite dike intruding the gabbroids. Zircons are large (>100 μm) and euhedral to subhedral; most show oscillatory zoning at the rim and unzoned cores. They contain 123–1357 ppm U, 42–659 ppm Th and have Th/U from 0.3 to 0.6 (Supplementary Document 3). The common-lead content is low, with $f_{206} = 0$–0.5%. Out of twenty-four analyses, nineteen define a concordia age of 531.2 ± 4.3 Ma (MSWD = 1.8; Fig. 5). This is taken as the crystallization age of this granodioritic dike. Five analyses show $^{206}Pb/^{238}U$ ages of *ca* 537 to 540 Ma.

4.2.5. Sample BR15-27

This is a medium-grained granite from the Bornavard granitoids. Zircons range from <50 μm to >100 μm and are prismatic; they contain 86–627 ppm U, 43–358 ppm Th and Th/U from 0.3 to 0.7 (Supplementary Document 3). Common lead is low, with $f_{206} = 0.03$–0.47%, except for point BR15-27@05; $f_{206} = 3.7\%$. Sixteen analyses give a concordia age of 552.2 ± 3.5 Ma (MSWD = 0.02; Fig. 5). This is the best estimate of the crystallization age of this sample. Zircons older than 560 Ma are interpreted as inherited grains.

4.2.6. Sample BR15-13

This is a coarse-grained granite from the Bornavard granitoids. Zircons range from 50 μm to 100 μm and are euhedral with stubby prismatic form. In CL images, they show oscillatory zoning around unzoned cores. They contain 112–742 ppm U, 61–522 ppm Th and have Th/U from 0.5–0.9. Twenty-two grains analyzed have low common Pb ($f_{206} = 0.01$–0.57%) except for point BR15-13@21 ($f_{206} = 1.27\%$). Fourteen analyses yield a concordia age of 547 ± 4 Ma (MSWD = 0.01; Fig. 5). Six analyses of cores yield a concordia age of 568 ± 6.1 Ma (not shown). One inherited core (point @16) is as old as >1.9 Ga (Supplementary Document 3). The zircon U–Pb ages of 552.2 ± 3.5 and 547 ± 4 Ma (within errors) are the best estimates of the crystallization age spectra of the Bornavard granites.

4.3. Zircon Hf–O isotopes

Granite zircons have heterogeneous $\delta^{18}O$, from 4.8 to 7.7‰ ($n = 40$; Fig. 6a); higher $\delta^{18}O$ values correlate with lower εHf. Most granitic zircons have O and Hf isotopes like those of juvenile, mantle-derived rocks. Inherited zircon cores have the same $\delta^{18}O$ values, as do 547–552 Ma zircons. Rhyolites have more homogeneous $\delta^{18}O$ values of 5.3–7.3‰ ($n = 20$, Fig. 6a), generally higher than zircons from granites (but with similar εHf values). The older granodioritic dike (sample BR15-24) has low $\delta^{18}O$ values, from 4.7 to 5.9‰, similar to juvenile zircons ($n = 20$, Fig. 6a), whereas the younger dike (sample BR15-41) has higher $\delta^{18}O$, from 5.4 to 10‰ ($n = 11$, Fig. 6a). Zircon oxygen isotopes are also heterogeneous in the gabbroic rocks ($\delta^{18}O = 5.5$–8.9‰; $n = 20$); zircons with higher $\delta^{18}O$ have lower εHf values.

Hf isotopic analyses were done on 111 grains from gabbroic, granitic, rhyolitic and granodioritic dike samples. Granites display a substantial range of εHf, between −1.6 and +6.9 (Fig. 6b). Inherited cores have similar εHf, varying between −1.6 (U–Pb age = 642 Ma) and −7.3 (U–Pb age = 1.9 Ga). Corresponding crustal model ages (T_{DM}^{C}) for all Taknar Cadomian granitic zircons vary from 0.9 to 1.5 Ga (average = 1.2 Ga). Rhyolites have more homogeneous εHf values, from +2 to +5 (Fig. 6b). T_{DM}^{C} of rhyolitic zircons varies between 1 and 1.2 Ga. Granodioritic dikes have more variable εHf, between −3.4 and +8.5 (Fig. 6b), with $T_{DM}^{C} = 1.1$–1.6 Ga. The lower εHf values (−3.4 to +4.3) are from the younger granodioritic dike. εHf values in gabbros vary between −3.1 and +7.4; crustal model ages are between 0.9 and 1.5 Ga (av. ~1.2 Ga).

4.4. Bulk rock major- and trace-element geochemistry

SiO_2 contents vary from 68–76 wt% in granitoids, 49–61% in gabbros–diorites, 69–73% in granodioritic dikes and ~76–80% in rhyolites (Supplementary Document 1). Mg# ($100Mg/(Mg + Fe^{+2})$) is very low in granitoids (3–10), but generally higher in granodioritic dikes (9–25) and rhyolites (6–17). Mg# is also high and variable in gabbros and diorites (12–32). K_2O is low in gabbros and diorites (0.6–1.8 wt.%) and in granodioritic dikes (0.2–1.2 wt.%), but increases in rhyolites (2.3–2.7 wt.%) and granitoids (3.2–4.1 wt.%).

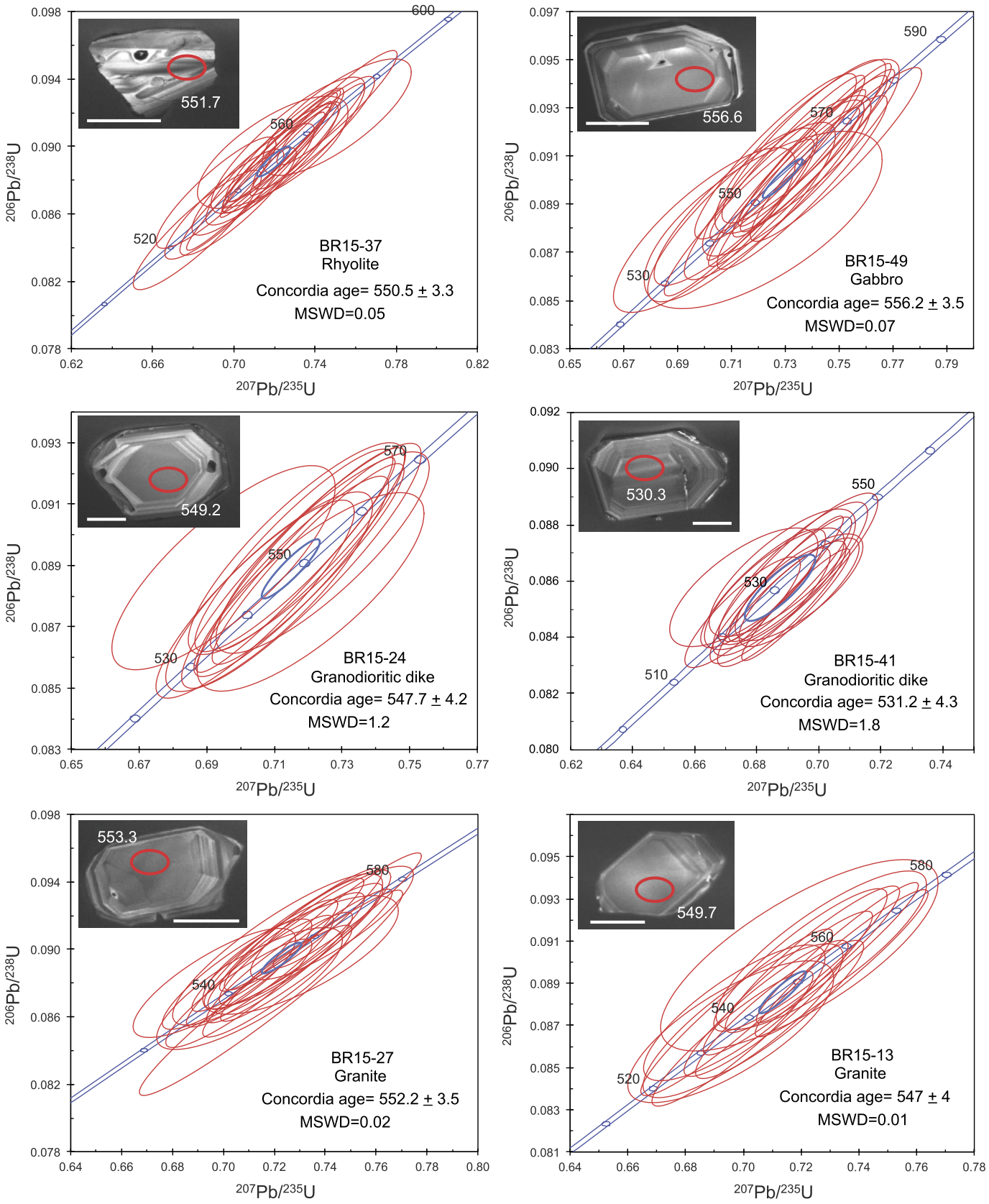

Fig. 5. SIMS U–Pb concordia age plots for the Taknar Cadomian granites, gabbros, rhyolites and granodioritic dikes.

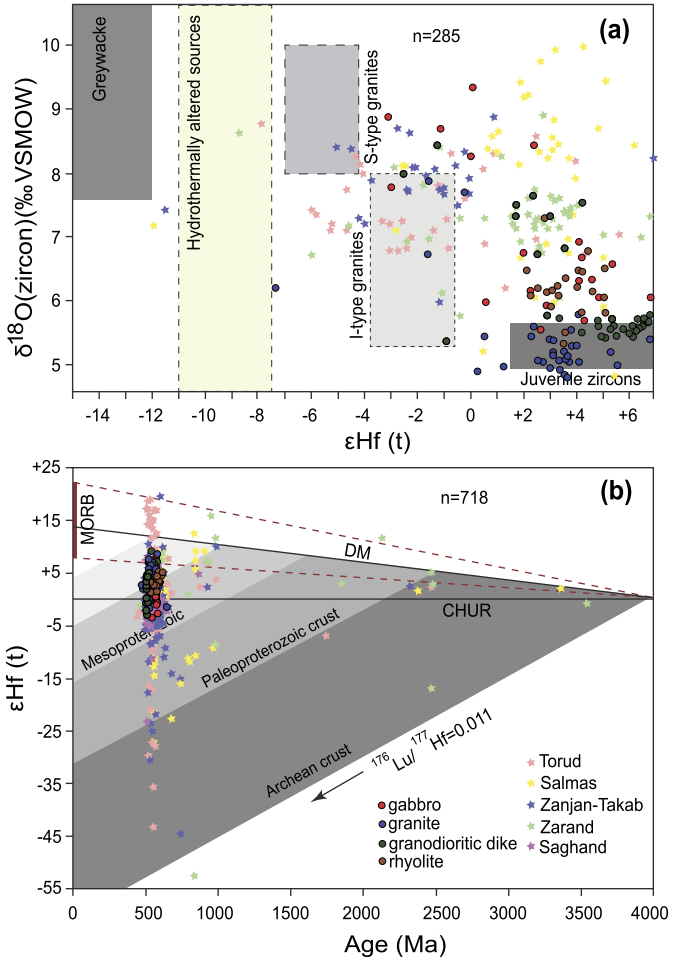

Fig. 6. (a) Plot of $\delta^{18}O$ *vs* $\varepsilon Hf(t)$ for Taknar Cadomian rocks (Modified after, Kemp et al., 2007). For comparison, data from Cadomian rocks of Torud, Salmas, Zanjan and Zarand are also shown (data from Moghadam et al., unpublished data and Moghadam et al., 2016b). (b) U–Pb age *vs* $\varepsilon Hf(t)$ plot for zircons from Taknar Cadomian rocks. Lu–Hf isotope data for Iran Cadomian rocks are from Moghadam et al. (unpublished data) excluding those for Torud Cadomian granites from Moghadam et al. (2015a, 2015b).

The large ion lithophile elements (LILEs) Ba, Rb, U and Th range between 42–871, 3–107, 0.24–4.2 and 0.8–20 ppm, respectively. Th/Yb ratios are low (0.3–2.1) but higher in other rocks (2.6–9.4). In the Th/Yb *vs* Nb/Yb plot (Leat et al., 2004) (Fig. 4b), all Cadomian rocks plot far above the mantle array, and the felsic magmatic rocks including granodioritic dikes, rhyolites and granitoids show Th/Yb ratios similar to upper crustal and/or shoshonitic rocks.

Concentrations of high-field strength elements (HFSEs) such as Nb and Y are low in the mafic rocks (12.1–12.3 and 19–47 ppm respectively), but higher in granitoids (10.8–15 and 49–67 ppm, respectively). In Nb *vs* Y and Yb + Nb diagrams (Pearce et al., 1984) (Figs. 4c and d), all the studied rocks (excluding granitoids) plot in the domain of volcanic arc granites (VAG), whereas the granitoids plot in the field of within-plate granites (WPG). REE patterns of granitoids and rhyolites (Fig. 7) show high La_n/Yb_n (2.9–5.7), and a conspicuous Eu negative anomaly. On a multi-element diagram (Fig. 7), these rocks exhibit positive anomalies for Rb, Ba, Th, U, K, Pb and negative anomalies in Ti, Sr, Ta and Nb relative to N-MORB. Granodioritic dikes are enriched in light REEs (La_n/Yb_n = 2.4–8.1) and slightly depleted in Eu, whereas gabbros and diorites are less enriched in LREEs (La_n/Yb_n = 1.4–6.1) and lack Eu anomalies (Fig. 7). Gabbroic rocks and granodioritic dikes are enriched in Th, U, K and Pb and depleted in Nb, Ta and Ti relative to the LREEs. Th–U enrichment is more obvious in granodioritic dikes than in gabbroic rocks. Zr and Hf are enriched in some gabbroids and granodioritic dikes, whereas other rocks are depleted (*e.g.*, Zr_n/Yb_n = 0.3–6.8) (Fig. 7). The geochemical signatures of Taknar rocks, including depletion in Nb, Ta, Ti, enrichment in Rb, Ba, Th, U, K, Pb and high LREE/HREE, resemble those of calc-alkaline igneous rocks of continental arcs (Ducea, 2002).

4.5. Bulk rock Sr–Nd isotopes

The initial $^{87}Sr/^{86}Sr$ (t = 550 Ma) of the Taknar Cadomian rocks ranges between 0.701 and 0.711. Samples with the same Nd-isotope ratios show different $^{87}Sr/^{86}Sr$. The unrealistically low value of BR15-4 (0.693; Supplementary Document 2) is linked to sericitization. If samples with $^{87}Rb/^{86}Sr > 5$ are excluded, the initial $^{87}Sr/^{86}Sr$ varies from 0.7030 to 0.7114; the lowest values are in gabbroic rocks. Nd isotopes are more resistant to alteration than Sr isotopes, and all Taknar magmatic rocks have both positive and negative $\varepsilon Nd(t)$ values; again, more juvenile compositions are found in gabbros. Granitoids have particularly low $\varepsilon Nd(t)$ values (−0.5 to −4.0) (Supplementary Document 2), which give depleted mantle model ages (T_{DM}) of 1.7–1.3 Ga. Rhyolites and granodioritic dikes have $\varepsilon Nd(t)$ of −0.4 to −1.4 with T_{DM} of ∼1.3–1.2 Ga. The gabbroic rocks have higher and more variable $\varepsilon Nd(t)$, ranging from −2.7 to +8.4. Gabbroic rocks clearly show more juvenile (mantle-derived) isotopic characteristics than do felsic rocks.

5. Discussion

5.1. Temporal and spatial distribution of Cadomian arcs

Cadomian magmatism affected large regions of present-day Europe, North Africa, NE parts of Arabia, Anatolia and Iran (Avigad et al., 2016; Moghadam et al., 2015a, 2015b) as well as parts of Tibet (Wang et al., 2016). Records of this event are found in a belt >5000 km long, from W Avalonia to Iran and Tibet (Fig. 1). Recent U–Pb–Hf–O studies on zircon in Cadomian rocks of western and southern Europe have been used to address the age and geochemical evolution of Cadomian magmatism. Sedimentary provenance analysis using U–Pb zircon ages has also proven useful (Avigad et al., 2015; Linnemann et al., 2014; Zlatkin et al., 2014). Although precise ages and isotopic data for Cadomian rocks in Europe are well established, U–Pb zircon ages and Hf–O isotopic analyses of Cadomian basement rocks from Iran and Turkey are less abundant.

Cadomian terranes in Iran and Turkey are dominated by metasediments, predominantly metamorphosed in amphibolite facies, and meta-igneous rocks especially granitic orthogneisses. Significant Cadomian magmatic exposures in Iran include: western (Golpayegan), northwestern (Khoy-Salmas, Zanjan-Takab), northeastern (Torud, Taknar) and central (Saghand) Iran (Fig. 2 and Supplementary Table 1). Unmetamorphosed Late Ediacaran–Early Cambrian intrusions and low-grade meta-sedimentary rocks outcrop widely in north and central Iran. Cadomian exposures are also scattered across Turkey, including the south (Poturge massif), west (Menderes and Sandikli massifs) and NW (Istanbul zone; Fig. 2).

The maximum sedimentation ages of Late Ediacaran–Early Paleozoic strata in western Cadomia are *ca* 588 to 536 Ma (Orejana et al., 2015). A similar age range of *ca* 573–537 Ma is reported from Late Ediacaran–Cambrian clastic sediments in Iran (Horton et al., 2008).

Cadomian mafic volcaniclastics, flows and sills are generally metamorphosed to amphibolite grade (Moghadam et al., 2015a, 2015b). Unmetamorphosed mafic rocks of Cadomian age are scarce, but are reported from Iberia (Orejana et al., 2015) and Turkey (Candan et al., 2015). Tholeiitic eclogites, thought to be

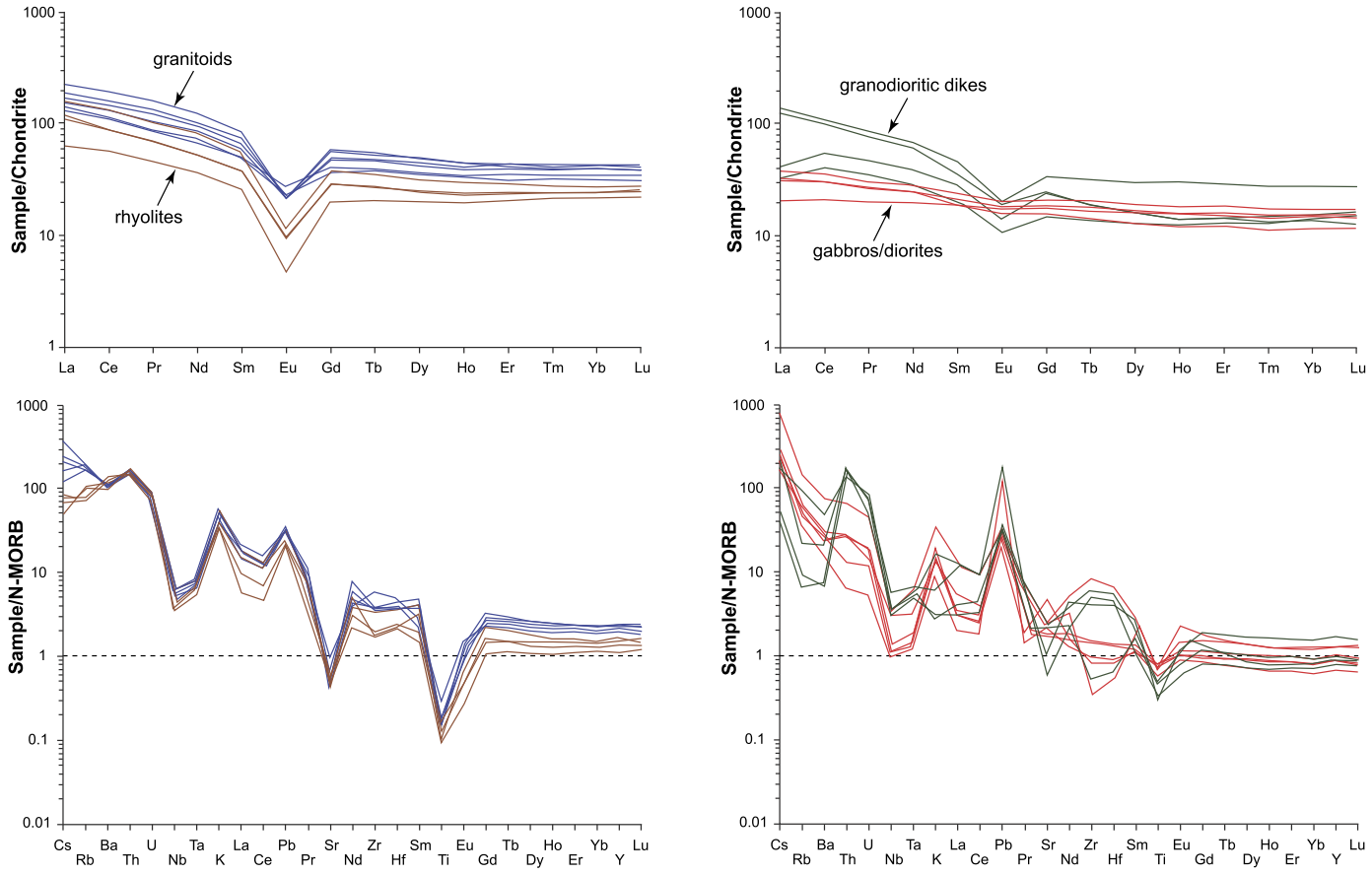

Fig. 7. Chondrite- and N-MORB-normalized rare earth and trace-element patterns for Taknar Cadomian rocks.

derived from a gabbroic protolith, are reported from the Menderes Massif of Turkey. These have *ca* 563 ± 1 Ma crystallization ages but were metamorphosed at 535 ± 3 Ma (Candan et al., 2015) and exhumed in a Cadomian subduction zone. Most other Cadomian basement rocks of Iran and Turkey were exhumed from the middle–lower crust during Cenozoic extension and formation of core complexes. Consequently, most Cadomian exposures in the region show Eocene–Oligocene partial melting that formed anatexite–diatexite and other melt-invasion features, or are intruded by Eocene–Miocene plutonic rocks (Moghadam et al., 2016a). Cadomian magmatic rocks in Iran and Turkey mostly are felsic plutons with minor dacitic extrusive rocks, and are best described as Volcanic Arc Granites (VAG) (Moghadam et al., 2015a, 2015b; Ustaomer et al., 2009). Bulk-rock Nd and zircon Hf–O isotopic data confirm that Cadomian melts comprise both juvenile additions to the crust and partial melts of continental crust (*e.g.*, Fig. 9d–e). The crustal melts may reflect subduction-related melting of thick continental crust underlying the Cadomian arc (Murphy et al., 2013).

Cadomian terranes in Europe were affected by the Hercynian (Variscan) orogeny and by magmatism of similar age (~320 Ma) in eastern domains, including Iran (Linnemann et al., 2008; Moghadam et al., 2015a, 2015b). Neoproterozoic–Cambrian sediments of the European Cadomian terranes may have been deposited in back-arc basins on thinned continental crust, flanked by the Cadomian magmatic arc to the north and by the craton (~2 Ga) of West Africa to the south (Linnemann et al., 2008) (Supplementary Appendix 1). The presence of MORB-like basalts, andesites, subordinate alkaline basalts with pillow structure, and black cherts in the Cadomian Bohemian massif may reflect back-arc spreading. Pelagic sediments and MORB-like magmatic associations are missing in Iran and Anatolia. This suggests that Cadomian activity in Anatolia–Iran did not occur in a backarc basin. This conclusion, and the observation that all Cadomian outcrops in Iran–Anatolia are felsic igneous rocks with arc geochemistry (*e.g.*, Fig. 4) and isotopic (*e.g.*, Fig. 6) signatures indicate the Cadomian igneous rocks of Iran and Anatolia formed in a continental magmatic arc that involved older crust. The existence of mafic magmatic rocks and tuffs in some Anatolia–Iran Cadomian outcrops indicates bimodal magmatic activity, which is well known from modern Andean-type arcs (*e.g.*, Ducea et al., 2015). Cadomian felsic rocks are also abundant in Iberia and Bohemia, but the mafic rocks are dominant and show Cadomian arc–oceanic back-arc assembly (*e.g.*, Fernandez et al., 2012; Murphy et al., 2013; von Raumer et al., 2015).

Zircon U–Pb ages from the Cadomian rocks of Iran and Turkey indicate that Cadomian magmatism took place between 500 and 600 Ma, with a high magmatic flux (flare-up) at *ca* 532–568 Ma in Iran and *ca* 524–576 Ma in Anatolia (Fig. 8a–b). Iranian and Anatolian Cadomian igneous rocks also share indistinguishable isotopic compositions (Fig. 9), suggesting that they comprise a single, coherent crustal block. The Cadomian of Iran–Anatolia thus is related to the Cadomian of Europe (Iberia and Bohemia, Fig. 8c–d) but magmatism started much earlier in the Europe, at ~670 Ma (Linnemann et al., 2008) and ended later. The data presented here in association with abundant studies on the Cadomian domains of Europe, also confirm that the Cadomian arc magmatism was a global igneous episode, but was diachronous from E to W.

As noted above, there is no evidence that the Cadomian crust of Iran and Turkey formed separately, and we conclude that the crust of Iran and Anatolia represents a single Cadomian block that rifted away from northern Gondwana during Late Paleozoic. Detrital–zircon surveys can also help us reconstruct the Late Neoproterozoic–Cambrian evolution of Iran and Anatolia. Fig. 8e–g

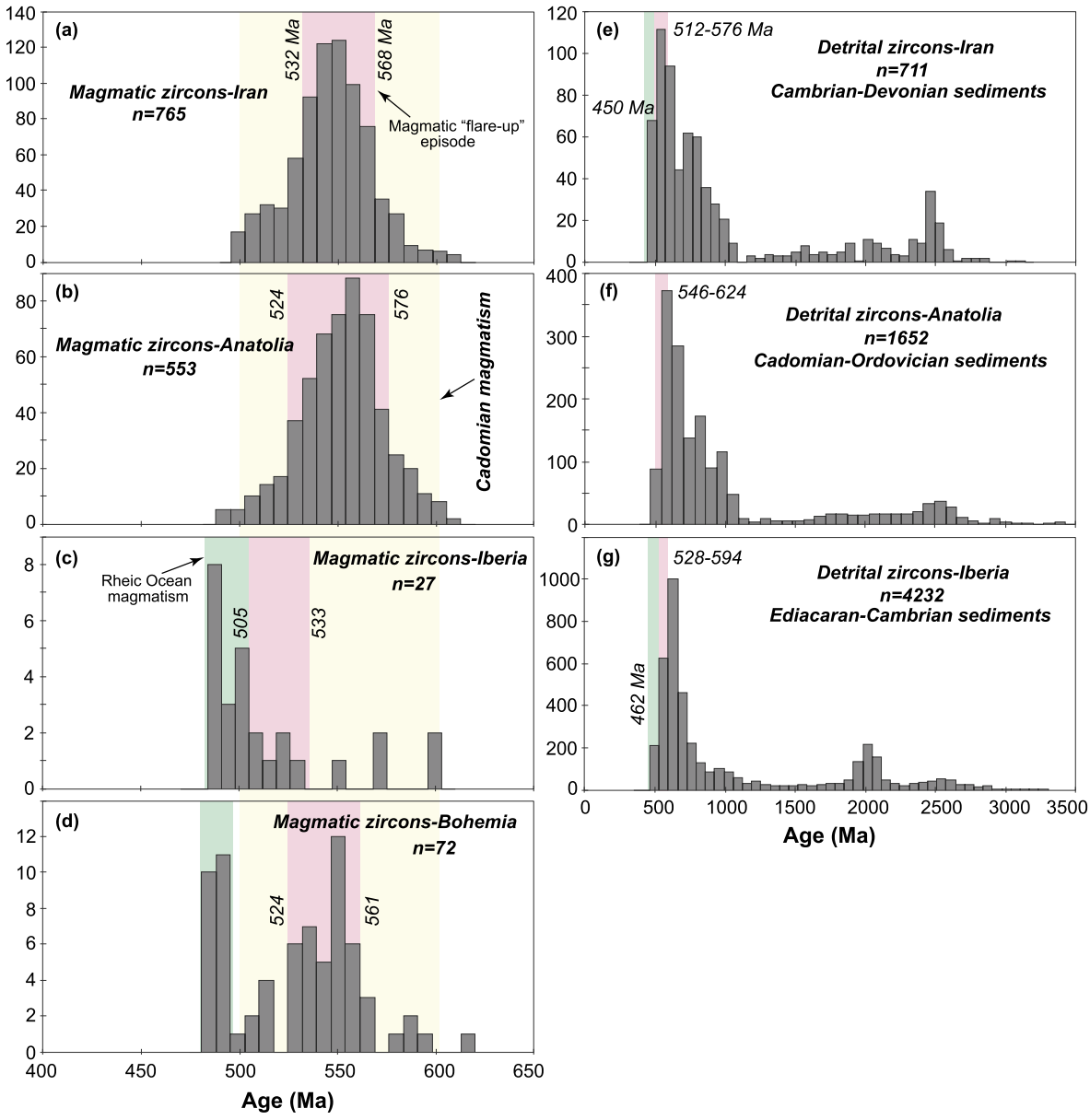

Fig. 8. Histograms showing the magmatic and detrital zircon age distribution of Cadomian rocks from Iran (a), Anatolia (b), Iberia (c) and Bohemia (d) as well as Cambrian–Devonian sediments of Iran (e), Cadomian–Ordovician sediments of Anatolia (f) and Cadomian sediments of Iberia (g). References for zircon U–Pb data from Iran and Turkey magmatic rocks are given in Supplementary Table 1. Data for Bohemia and Iberia magmatic zircons are from Andonaegui et al. (2012) and Fernandez et al. (2012) respectively. Detrital–zircon data for Iranian sediments are from Moghadam et al. (unpublished data, 2017), Anatolian sediments from Zlatkin et al. (2013) and Iberian sediments from Fernandez-Suarez et al. (2014), Orejana et al. (2015), Pereira et al. (2012).

compiles detrital-zircon ages from Cambrian–Devonian sediments of Iran, Cadomian–Ordovician sediments of Anatolia and Cadomian sedimentary rocks of Iberia (see Fig. 8 caption for references). These sediments are dominated by Neoproterozoic and Cambrian zircons but also contain Archean zircons in Anatolia–Iran and Paleoproterozoic zircons in Iberia, which serve to distinguish Anatolia–Iran from Iberia. The zircon age spectra indicate that the Cadomian flare-up occurred in Iran at *ca* 512–576 and that these igneous rocks were the dominant contributor to the sediments. In both Iran and Anatolia, juvenile igneous rocks of the Arabian–Nubian Shield (580–1000 Ma) were also an important sediment source.

Significant amounts of sediments, interpreted as deposited in Cadomian intra-arc basins, were predominantly (>90%) derived from erosion of local Cadomian rocks (Balaghi et al., 2014; Moghadam et al., 2015a, 2015b). The maximum age of sedimentation is variable and overlaps in time with the local magmatism. Cadomian sediments were also deposited in a retro-arc basin between the continental arc and the passive margin, and thus contain Archean as well as Neoproterozoic zircons (Fig. 8e). Younger granitic plutons crosscut both older intrusions and sedimentary sequences, *e.g.*, 522 Ma granites from NE Iran (Torud, Fig. 2), injected into older (540–560 Ma) metamorphosed plutonic rocks and sediments (Moghadam et al., 2016b).

Some Cadomian exposures in Iran are disconformably covered by weakly- or unmetamorphosed Cambrian–Ordovician sediments, with zircon age peaks of 450–492 Ma (this study and Moghadam et al., 2017) that can reflect magmatism and sedimentation in a rift basin related to the opening of Paleotethys (*e.g.*, Stampfli et al., 1991). Cambro-Ordovician deposits of NE Iran including Zagun, Lalun and upper parts of the Mila Formation contain widespread mafic-intermediate sills/lavas, which are examples of Paleotethys-

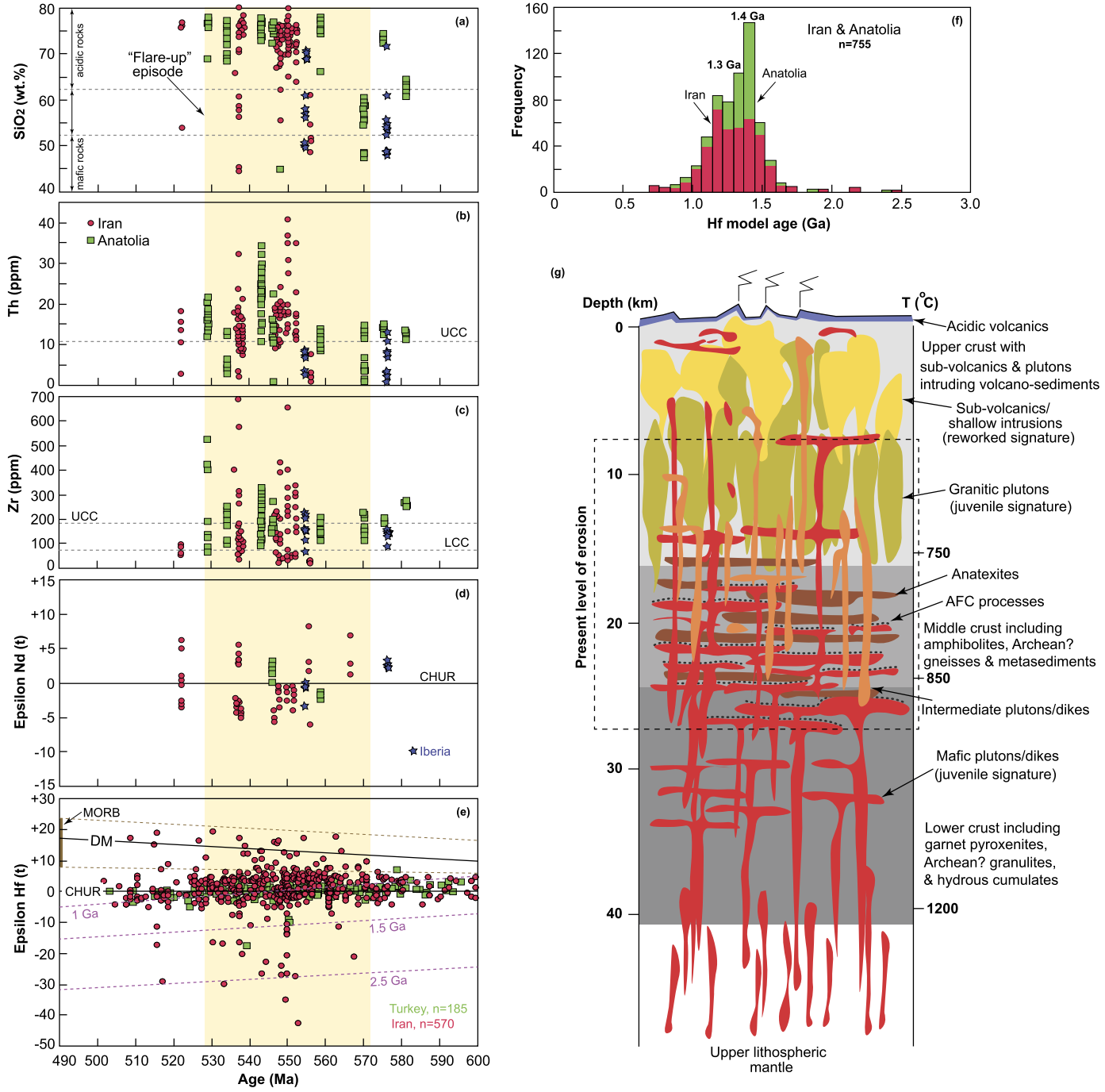

Fig. 9. Evolution plots of (a) SiO_2, (b) Th, (c) Zr and (d) and (e) isotopic (bulk rock Nd and zircon Hf) geochemistry of the Cadomian magmatism time for Iran and Anatolia igneous rocks. The composition of upper (UCC) and lower continental crusts (LCC) are from Taylor and Mclennan (1995). CHUR = chondrite normalized uniform reservoir; DM = depleted mantle array (based on data from modern Mid-Oceanic Ridge basalts with $^{176}Hf/^{177}Hf = 0.28325$ and using $^{176}Lu/^{177}Hf = 0.0384$ (Chauvel and Blichert-Toft, 2001). (f) Zircon Hf crustal model ages for all Cadomian rocks from Iran and Anatolia. See Supplementary Table 1 for references of Iran and Anatolia Cadomian rocks data. Data for Iberia Cadomian rocks are from Bandres et al. (2004). (g) A schematic crustal column through the Cadomian arcs of Iran and Anatolia.

related rift magmatism that could have provided 490–450 Ma detrital zircons. However, the existence of the Paleotethys Ocean between the European Variscan autochthonous domains and the north Gondwana margin has been questioned based on paleontological constraints (Shaw and Johnston, 2016). Both stratigraphy (Aharipour et al., 2009) and detrital zircon survey (Moghadam et al., 2017) show that Paleotethys was present on the eastern side of north Gondwana.

The lifespan of the Cadomian arcs ranged from ~180 Myr in the west (Europe) (*e.g.* Linnemann et al., 2008) to ~<100 Myr in the east (Iran–Anatolia) (*e.g.*, Moghadam et al., 2015a, 2015b). Early Cadomian magmatism overlaps the last phases of Pan-African juvenile magmatism in the 580–900 Ma Arabian–Nubian Shield (ANS) and late Cadomian activity overlaps with Early Paleozoic magmatism (<500 Ma) linked to opening of the Rheic ocean. Cadomian subduction zone and associated continental arcs formed after continental collision beginning ~630 Ma to form Greater Gondwana (Johnson et al., 2013). After the collision, the Prototethys margin collapsed beneath northern Gondwana to cause the initiation of southward subduction and to nucleate the Cadomian arcs now found in Europe and then propagated to the east. Cadomian arc magmatism died out at ~490–480 Ma in the west and

~520–500 Ma in the east. It is not clear why the Cadomian arcs shut down, but the end of subduction at ~540–500 Ma may be related to opening of the Rheic Ocean (Linnemann et al., 2007b; Murphy et al., 2006). The change in plate tectonic setting may reflect ridge–continent collision and slab break-off, which switched Cadomian arcs from an active margin to a transform margin (Linnemann et al., 2007a).

5.2. Petrogenesis and magmatic sources of Cadomian igneous rocks

Taknar igneous rocks are enriched in LREEs and in Rb, Ba, Th, U, Pb and K, and depleted in Nb, Ta, Ti; this signature is characteristic of subduction-related magmas. Plots of Th/Yb *vs* Nb/Yb (Fig. 4b) and Nb *vs* Y and Y + Nb (Fig. 4c–d) further support a magmatic-arc origin for these rocks. This signature also is typical of all Cadomian igneous rocks from Iran and Anatolia (Fig. 4). High concentrations of Th in Taknar rocks (and hence high Th/Yb ratios) associated with negative $\varepsilon Nd(t)$ (−0.4 to −4, excluding gabbros with $\varepsilon Nd(t) = +1.5$ to +8.4) show high contributions of crustal materials during the genesis and evolution of the Taknar magmas. Nd-isotope crustal residence ages (T_{DM}) of Taknar rocks range from 1.2–1.7 Ga, indicating that continental crust at least as old as Mesoproterozoic was involved. Taknar zircons display a range of εHf between −3.4 and +8.5 with $T_{DM}{}^{C}$ of 0.9–1.5 Ga. Nd isotopic data indicate a similar source; rhyolites and granodioritic dikes have $\varepsilon Nd(t)$ of −0.44 to −1.4 with T_{DM} of ~1.3–1.2 Ga. In contrast to the felsic rocks, the Taknar gabbroic rocks have higher and more variable $\varepsilon Nd(t)$ (−2.7 to 8.4). This suggests that the genesis of the felsic magmas involved assimilation of significant volumes of older continental crust. Because pre-Cadomian rocks are unknown from Anatolia–Iran, Cadomian magmatism must have entailed pervasive melting of older continental crust during magma-crust interaction and contamination. Oxygen isotopic compositions show less evidence for involvement of older continental crust. Elevated zircon $\delta^{18}O$ in igneous rocks ($\delta^{18}O > 7‰$) also requires the involvement of supracrustal rocks; arc rocks from continental active margins usually have $\delta^{18}O$ of ~8.5‰. Zircon $\delta^{18}O$ from Taknar granites (*av*. 5.4‰), rhyolites (*av*. 6.2‰), granodioritic dikes (*av*. 6.5‰) and even gabbros (*av*. 6.8‰) thus are lower than expected for arc continental rocks. Involvement of lower continental crust can best explain Nd, Hf, and O isotopic data for Taknar igneous rocks, but not trace element data as discussed below.

To better understand magmagenesis in the Cadomian arc of Iran and Anatolia, we compiled major elements, incompatible trace elements and isotopes for this region. The Cadomian arc of Iran–Anatolia has largely been eroded to plutonic levels, so their volcanic counterparts (upper crust) are preserved only locally such as the Taknar complex (*this study*) or the Derik volcanics in S Anatolia. The lower parts of the upper to middle Cadomian crust in Iran–Anatolia consist mostly of granitoids. Juvenile mafic rocks include cumulate olivine + orthopyroxene metagabbros of Torud, NE Iran. In this mid- to deep crustal level, as in other continental arcs world-wide (Ducea et al., 2010), gabbros with high zircon εHf reflect juvenile additions from the mantle (Moghadam et al., unpublished data). SiO_2 abundances for Iran–Anatolia Cadomian rocks (Fig. 9a) are variable but >85% have >62 wt% silica, as do granodiorite-granites in modern continental arcs (Ducea et al., 2015).

The compiled compositional data suggest that Cadomian magma generation and differentiation occurred above a subduction zone beneath a thin, extensional Andean-type convergent margin. Differentiation and assimilation-fractional crystallization increased incompatible elements such as Th and Zr in the evolving melts. The abundance of Th and Zr in upper and lower continental crust is 10.7 and 190 ppm and 1.1 and 70 ppm respectively (Taylor and Mclennan, 1995). The data show that >90% of Cadomian rocks from Iran–Anatolia have Zr abundances higher than expected for lower continental crust (Fig. 9c). Th concentrations in Cadomian rocks are even higher than in typical upper continental crust (Fig. 9b). High whole-rock Th concentrations of Iran–Anatolia Cadomian rocks (as well as whole-rock Nd and zircon Hf isotope data for most of the rocks) show interaction of Cadomian juvenile basaltic melts with older continental crust, consistent with the negative εNd values of most Cadomian igneous rocks in Iran–Anatolia (Fig. 9d). Cadomian rocks from Iberia also have bimodal major element compositions and are mostly characterized by low Th and Zr abundances, similar to inferred Cadomian lower crust of Iran–Anatolia. Zircon εHf for Iranian rocks (~470 grains, ~50 samples) ranges from juvenile (+18.7) to values expected for old crust (−43), but ~91% of the zircons have εHf between −9.6 and +10.7 (Fig. 9e). Zircon εHf for Anatolia ($n = 185$) ranges from −45 to +7, and 98% are between −9.5 and +7. This range of Hf and Nd data clearly shows involvement of both juvenile melts and variable-aged continental crust during the Cadomian "flare-up" (~528–572 Ma) in Iran–Anatolia, and reflects the interplay between the fractionating basaltic mantle-derived melts and the old continental crust (*e.g.*, Ducea et al., 2015).

The depth of fractionation can affect some whole rock elemental ratios such as Sr/Y and/or $La_{(n)}/Yb_{(n)}$. Chapman et al. (2015) and Profeta et al. (2015) hypothesized that Sr/Y and $La_{(n)}/Yb_{(n)}$ elemental ratios can be used as crustal thickness proxies for intermediate calc-alkaline rocks (55–68 wt% SiO_2). Our compiled data show that most of the Cadomian rocks are highly fractionated and have high SiO_2 content (>70 wt%). However, considering Cadomian rocks with intermediate SiO_2 composition (55–68 wt% SiO_2), we found that the crustal thickness or Moho depth (using equation provided by Profeta et al., 2015) is in the range of 20 to 30 km, which is less than might be expected for a Cadomian continental arc unless it was strongly extensional. We consider this shallow depth (20–30) as the latest fractionation depth, which allows plagioclase to dominate fractionation, as required by the observation that most rocks have negative Eu and Sr anomalies. Inherited older zircons found in most Cadomian igneous rocks testifies to shallow crustal fractionation and assimilation.

The age of the continental crust assimilated during the Cadomian flare-up is debatable. Zircon εHf values indicate that Paleoproterozoic crust is a candidate (Fig. 6b), but ~5% of zircons also have Archean (2.5 Ga) Hf model ages. The $T_{DM}{}^{C}$ histogram (Fig. 9f) shows minimum ages of 1.3–1.4 Ga for the old continental crust involved in assimilation. Fig. 6b shows few inherited zircons with this age (1.3–1.4 Ga) in Cadomian rocks, but instead 2.5 Ga inherited zircons are present. Archean inherited zircons may come from the underlying passive margin of Gondwana on which the Cadomian arc was constructed. Detrital zircon populations from Iran and Anatolia (Fig. 8e–f) also contain many Archean zircons, but these do not require underlying Archean crust; they could also come from the older sedimentary rocks derived from Gondwana. *In situ* examples of the old continental crust have not been recognized in the Bohemia and Iberian segments of Cadomia, but both Tonian (~1 Ga) and Archean (2.5 Ga) crusts have been suggested (Dorr et al., 2015; Linnemann et al., 2008).

5.3. Triggers of the Cadomian magmatic "flare-up"

The Cadomian magmatic arc was affected by high magma fluxes during a ~44 million year-long (528–572 Ma) flare-up in Iran and Anatolia. Although more geologic mapping and geochronology is needed in order to estimate magma fluxes, available data show that a ~2000 km long and ~50 km wide arc magmatic belt was produced as Prototethys subducted southwards beneath northern Gondwana (Supplementary Appendix 1). This implies that the apparent intrusive rate (surface area per time) during the Cadomian

flare-up was ~2300 km^2/Myr in Iran and Anatolia; if we assume that the crust was 40 km thick, this results in a magmatic volume of 92,000 km^3/Myr. This is a much higher magma production rate and a much greater total volume than for North American arcs (~1000 km^2/Myr for a ~20 Myr flare-up, again assuming crust 40 km thick = 40,000 km^3/Myr (Ducea et al., 2015)). This flare-up generated ~90% of the Cadomian crust of Iran–Anatolia.

What caused the Cadomian flare-up in Iran and Anatolia? Prototethys slab retreat may have caused extension of lithosphere above the subduction zone, which would have enhanced magmatic productivity. However, ridge-continent collision and slab break-off also may have changed the active margin to a transform margin in the western (European) Cadomian arcs (Linnemann et al., 2007a). Because there are no Cadomian adakites in Iran–Turkey, we see no evidence for ridge subduction or subduction of young oceanic crust.

There are three lines of evidence for an extensional tectonic regime for the Cadomian arcs of Turkey and Iran, which could have been caused by slab retreat or delamination. First, juvenile mafic-intermediate magmas and felsic crustally-derived magmas occurred simultaneously during Iran–Anatolia Cadomian arc activity. Cadomian mafic plutonic rocks from Iran have juvenile signatures (*e.g.*, high εNd and εHf) but differ from MORBs (with whole rock εNd = *av.* + 12 and zircon εHf = *av.* + 16), suggesting involvement of Cadomian sub-continental mantle (Balaghi et al., 2014). These lines of evidence suggest that the convective removal of lithosphere may have triggered the Cadomian flare-up. Second, slab retreat and extension are thought to have been responsible for back-arc basin formation in Europe (Rheic Ocean, Nance et al., 2010) and a series of the extensional basins in Iran and Turkey. These basins accumulated several kilometers of sediments, depending on whether they received more distal and ancient sediments (*e.g.*, detritus from the West African Craton, to Europe) or local Cadomian detritus, as in Iran (Fernandez et al., 2012; Fernandez-Suarez et al., 2014; Horton et al., 2008; Moghadam et al., 2017; Orejana et al., 2015; Pereira et al., 2012). Third, a Cadomian extensional regime explains exhumation and uplift of the arc as well as partial melting and formation of diatexites, which are widespread in Cadomian exposures of Iran (*e.g.*, Moghadam et al., 2015a, 2015b); in Anatolia, even Cadomian eclogites were exhumed (Candan et al., 2015). These slab-retreat-related characteristics are consistent with more recent analogues, especially those described from North American arc (*e.g.*, Ducea and Saleeby, 1998) and the Andean arc of South America (*e.g.*, Ducea et al., 2015).

In summary, isotopic and trace-element signatures provide strong evidence that the magmas of the Cadomian flare-up in Iran and Anatolia were derived primarily from the upper plate, i.e., sub-continental mantle and overlying crust. This led to a crude stratification in Cadomian arcs, composed from bottom to top of: 1) two pyroxene + olivine ± amphibole cumulates (and/or their metamorphic equivalents, mafic amphibolites) and garnet pyroxenites in the lower crust; 2) felsic (granitoid)-rich middle crust and 3) volcanic-sedimentary upper crust (*e.g.*, Balaghi et al., 2014; Moghadam et al., 2016b; Stern et al., 2016) (Fig. 9g). The data presented here suggest that a preexisting lower–middle crust (probably Archean) underlay the Iran–Anatolia Cadomian arcs and that this old crust contributed significantly to Cadomian magmas. As in the case of modern arcs, material supplied by subduction erosion could also have been a major contributor to the arc magma budget, but it is difficult to isotopically distinguish this process from magmatic assimilation of much older continental crust.

6. Conclusions

A magmatic flare-up triggered voluminous arc magmatism and rapid continental growth along the northern margin of Gondwana beginning at ~572 Ma and lasting for ~44 million years. Taknar magmatism of NE Iran with U–Pb ages of ~556–531 Ma was part of this flare-up. A survey of trace elements, bulk-rock Nd isotopes and zircon Hf-isotope compositions indicates the involvement of both juvenile melts and older continental crust in the generation of the Iran–Anatolia Cadomian rocks. Cadomian arc magmatism was associated with subduction of the Prototethys Ocean beneath northern Gondwana and was linked with backarc extension. Convective removal of the lithosphere (delamination) probably triggered the Cadomian high-flux event.

Acknowledgements

This study was funded by the Chinese Academy of Sciences (grants XDB18000000 and 2015VEC063). Sr and Nd isotopic analyses were done in the scope of project Geobiotec (UID/GEO/04035/2013), funded by FCT (Portugal). This is contribution 972 from the ARC Centre of Excellence for Core to Crust Fluid Systems (http://www.ccfs.mq.edu.au), 1155 in the GEMOC Key Centre (http://www.gemoc.mq.edu.au), and 1300 from UTD Geosciences. All logistical support for field studies in NE Iran came from Damghan University.

Appendix. Supplementary material

Supplementary material related to this article can be found online at http://dx.doi.org/10.1016/j.epsl.2017.06.028.

References

Abbo, A., Avigad, D., Gerdes, A., Gungor, T., 2015. Cadomian basement and Paleozoic to Triassic siliciclastics of the Taurides (Karacahisar dome, south-central Turkey): paleogeographic constraints from U–Pb–Hf in zircons. Lithos 227, 122–139.

Aharipour, R., Moussavi, M.R., Mosaddegh, H., Mistiaen, B., 2009. Facies features and paleoenvironmental reconstruction of the Early to Middle Devonian syn-rift volcano-sedimentary succession (Padeha Formation) in the Eastern-Alborz Mountains, NE Iran. Facies 56, 279–294.

Andonaegui, P., Castineiras, P., Cuadra, P.G., Arenas, R., Martinez, S.S., Abati, J., Garcia, F.D., Catalan, J.R.M., 2012. The Corredoiras orthogneiss (NW Iberian Massif): geochemistry and geochronology of the Paleozoic magmatic suite developed in a peri-Gondwanan arc. Lithos 128, 84–99.

Avigad, D., Abbo, A., Gerdes, A., 2016. Origin of the Eastern Mediterranean: neotethys rifting along a cryptic Cadomian suture with Afro-Arabia. Geol. Soc. Am. Bull.. B31370.31371.

Avigad, D., Weissbrod, T., Gerdes, A., Zlatkin, O., Ireland, T.R., Morag, N., 2015. The detrital zircon U–Pb–Hf fingerprint of the northern Arabian–Nubian Shield as reflected by a Late Ediacaran arkosic wedge (Zenifim Formation; subsurface Israel). Precambrian Res. 266, 1–11.

Bagherzadeh, R.M., Karimpour, M.H., Farmer, G.L., Stern, C.R., Santos, J.F., Rahimi, B., Heidarian Shahri, M.R., 2015. U–Pb zircon geochronology, petrochemical and Sr–Nd isotopic characteristic of Late Neoproterozoic granitoid of the Bornaward Complex (Bardaskan, NE Iran). J. Asian Earth Sci. 111, 54–71.

Balaghi, M.E., Mahmoud, S., Zhai, M.G., Habibollah, G., Mohammad, M., 2014. Zircon U–Pb ages, Hf isotopes and geochemistry of the schists, gneisses and granites in Delbar Metamorphic-Igneous Complex, SE of Shahrood (Iran): implications for Neoproterozoic geodynamic evolutions of Central Iran. J. Asian Earth Sci. 92, 92–124.

Balintoni, I., Balica, C., Ducea, M.N., Hann, H.P., Sabliovschi, V., 2010. The anatomy of a Gondwanan terrane: the Neoproterozoic–Ordovician basement of the pre-Alpine Sebes-Lotru composite terrane (South Carpathians, Romania). Gondwana Res. 17, 561–572.

Bandres, A., Eguiluz, L., Pin, C., Paquette, J.L., Ordonez, B., Le Fevre, B., Ortega, L.A., Ibarguchi, J.I.G., 2004. The northern Ossa-Morena Cadomian batholith (Iberian Massif): magmatic arc origin and early evolution. Int. J. Earth Sci. 93, 860–885.

Candan, O., Koralay, O.E., Topuz, G., Oberhänsli, R., Fritz, H., Collins, A.S., Chen, F., 2015. Late Neoproterozoic gabbro emplacement followed by early Cambrian eclogite-facies metamorphism in the Menderes Massif (W. Turkey): implications on the final assembly of Gondwana. Gondwana Res. 34, 158–173.

Chapman, J.B., Ducea, M.N., DeCelles, P.G., Profeta, L., 2015. Tracking changes in crustal thickness during orogenic evolution with Sr/Y: an example from the North American Cordillera. Geology 43, 919–922.

Chauvel, C., Blichert-Toft, J., 2001. A hafnium isotope and trace element perspective on melting of the depleted mantle. Earth Planet. Sci. Lett. 190, 137–151.

Dorr, W., Zulauf, G., Gerdes, A., Lahaye, Y., Kowalczyk, G., 2015. A hidden Tonian basement in the eastern Mediterranean: age constraints from U–Pb data of magmatic and detrital zircons of the External Hellenides (Crete and Peloponnesus). Precambrian Res. 258, 83–108.
Ducea, M.N., 2002. Constraints on the bulk composition and root foundering rates of continental arcs: a California arc perspective. J. Geophys. Res., Solid Earth 107.
Ducea, M.N., Barton, M.D., 2007. Igniting flare-up events in Cordilleran arcs. Geology 35, 1047–1050.
Ducea, M.N., Otamendi, J.E., Bergantz, G., Stair, K.M., Valencia, V.A., Gehrels, G.E., 2010. Timing constraints on building an intermediate plutonic arc crustal section: U–Pb zircon geochronology of the Sierra Valle Fertil-La Huerta, Famatinian arc, Argentina. Tectonics 29.
Ducea, M., Saleeby, J., 1998. A case for delamination of the deep batholithic crust beneath the Sierra Nevada, California. Int. Geol. Rev. 40, 78–93.
Ducea, M.N., Saleeby, J.B., Bergantz, G., 2015. The architecture, chemistry, and evolution of continental magmatic arcs. Annu. Rev. Earth Planet. Sci. 43 (43), 299–331.
Fernandez, R.D., Castineiras, P., Barreiro, J.G., 2012. Age constraints on Lower Paleozoic convection system: magmatic events in the NW Iberian Gondwana margin. Gondwana Res. 21, 1066–1079.
Fernandez-Suarez, J., Gutierrez-Alonso, G., Pastor-Galan, D., Hofmann, M., Murphy, J.B., Linnemann, U., 2014. The Ediacaran–Early Cambrian detrital zircon record of NW Iberia: possible sources and paleogeographic constraints. Int. J. Earth Sci. 103, 1335–1357.
Gursu, S., Moller, A., Goncuoglu, M.C., Koksal, S., Demircan, H., Koksal, F.T., Kozlu, H., Sunal, G., 2015. Neoproterozoic continental arc volcanism at the northern edge of the Arabian Plate, SE Turkey. Precambrian Res. 258, 208–233.
Horton, B.K., Hassanzadeh, J., Stockli, D.F., Axen, G.J., Gillis, R.J., Guest, B., Amini, A., Fakllari, M.D., Zamanzadeh, S.M., Grove, M., 2008. Detrital zircon provenance of Neoproterozoic to Cenozoic deposits in Iran: implications for chronostratigraphy and collisional tectonics. Tectonophysics 451, 97–122.
Johnson, P.R., Halverson, G.P., Kusky, T.M., Stern, R.J., Pease, V., 2013. Volcanosedimentary basins in the Arabian–Nubian Shield: markers of repeated exhumation and denudation in a Neoproterozoic accretionary orogen. Geosciences 3, 389–445.
Kemp, A.I.S., Hawkesworth, C.J., Foster, G.L., Paterson, B.A., Woodhead, J.D., Hergt, J.M., Gray, C.M., Whitehouse, M.J., 2007. Magmatic and crustal differentiation history of granitic rocks from Hf–O isotopes in zircon. Science 315, 980–983.
Leat, P.T., Pearce, J.A., Barker, R.F., Millar, I.L., Barry, T.L., Larter, R.D., 2004. Magma genesis and mantle flow at a subducting slab edge: the South Sandwich arc-basin system. Earth Planet. Sci. Lett. 227, 17–35.
Linnemann, U., Gerdes, A., Drost, K., Buschmann, B., 2007a. The continuum between Cadomian orogenesis and opening of the Rheic Ocean: constraints from LA-ICP-MS U–Pb zircon dating and analysis of plate-tectonic setting (Saxo-Thuringian zone, northeastern Bohemian Massif, Germany). In: Evolution of the Rheic Ocean: From Avalonian–Cadomian Active Margin to Alleghenian–Variscan Collision. In: GSA Special Papers, vol. 423, pp. 61–96.
Linnemann, U., Gerdes, A., Hofmann, M., Marko, L., 2014. The Cadomian Orogen: Neoproterozoic to Early Cambrian crustal growth and orogenic zoning along the periphery of the West African Craton-Constraints from U–Pb zircon ages and Hf isotopes (Schwarzburg Antiform, Germany). Precambrian Res. 244, 236–278.
Linnemann, U., Nance, R.D., Kraft, P., Zulauf, G., 2007b. Preface. In: Evolution of the Rheic Ocean: From Avalonian-Cadomian Active Margin to Alleghenian–Variscan Collision. In: GSA Special Papers, vol. 423, pp. VII–VIII.
Linnemann, U., Ouzegane, K., Drareni, A., Hofmann, M., Becker, S., Gartner, A., Sagawe, A., 2011. Sands of West Gondwana: an archive of secular magmatism and plate interactions – a case study from the Cambro–Ordovician section of the Tassili Ouan Ahaggar (Algerian Sahara) using U–Pb–LA–ICP–MS detrital zircon ages. Lithos 123, 188–203.
Linnemann, U., Pereira, F., Jeffries, T.E., Drost, K., Gerdes, A., 2008. The Cadomian Orogeny and the opening of the Rheic Ocean: the diacrony of geotectonic processes constrained by LA–ICP–MS U–Pb zircon dating (Ossa-Morena and Saxo-Thuringian Zones, Iberian and Bohemian Massifs). Tectonophysics 461, 21–43.
Linnemann, U., Romer, R.L., Gerdes, A., Jeffries, T.E., Drost, K., Ulrich, J., 2010. The Cadomian Orogeny in the Saxo-Thuringian Zone. In: Linnemann, U., Romer, R.L. (Eds.), Pre-Mesozoic Geology of Saxo-Thuringia – From the Cadomian Active Margin to the Variscan Orogen. Schweizerbart, Stuttgart, pp. 37–58.
Moghadam, H.S., Khademi, M., Hu, Z.C., Stern, R.J., Santos, J.F., Wu, Y.B., 2015a. Cadomian (Ediacaran–Cambrian) arc magmatism in the ChahJam–Biarjmand metamorphic complex (Iran): magmatism along the northern active margin of Gondwana. Gondwana Res. 27, 439–452.
Moghadam, H.S., Li, X.-H., Ling, X.-X., Stern, R.J., Khedr, M.Z., Chiaradia, M., Ghorbani, G., Arai, S., Tamura, A., 2015b. Devonian to Permian evolution of the Paleo-Tethys Ocean: new evidence from U–Pb zircon dating and Sr–Nd–Pb isotopes of the Darrehanjir–Mashhad "ophiolites", NE Iran. Gondwana Res. 28, 781–799.
Moghadam, H.S., Li, X.-H., Griffin, W.L., Stern, R.J., Thomsen, T.B., Meinhold, G., Aharipour, R., O'Reilly, S.Y., 2017. Early Paleozoic tectonic reconstruction of Iran: tales from detrital zircon geochronology. Lithos 268, 87–101.
Moghadam, H.S., Li, X.-H., Stern, R.J., Ghorbani, G., Bakhshizad, F., 2016a. Zircon U–Pb ages and Hf–O isotopic composition of migmatites from the Zanjan–Takab complex, NW Iran: constraints on partial melting of metasediments. Lithos 240–243, 34–48.
Moghadam, H.S., Li, X.H., Stern, R.J., Santos, J.F., Ghorbani, G., Pourmohsen, M., 2016b. Age and nature of 560–520 Ma calc-alkaline granitoids of Biarjmand, northeast Iran: insights into Cadomian arc magmatism in northern Gondwana. Int. Geol. Rev. 58, 1492–1509.
Muller, R., Walter, R., 1983. Geology of the Precambrian–Paleozoic Taknar Inliers Northwest of Kashmar, Khorasan Province, NE Iran. GSI Reports, 165–183.
Murphy, J.B., Gutierrez-Alonso, G., Nance, R.D., Fernandez-Suarez, J., Keppie, J.D., Quesada, C., Strachan, R.A., Dostal, J., 2006. Origin of the Rheic Ocean: rifting along a Neoproterozoic suture? Geology 34, 325–328.
Murphy, J.B., Pisarevsky, S., Nance, R.D., 2013. Potential geodynamic relationships between the development of peripheral orogens along the northern margin of Gondwana and the amalgamation of West Gondwana. Mineral. Petrol. 107, 635–650.
Nance, R.D., Gutierrez-Alonso, G., Keppie, J.D., Linnemann, U., Murphy, J.B., Quesada, C., Strachan, R.A., Woodcock, N.H., 2010. Evolution of the Rheic Ocean. Gondwana Res. 17, 194–222.
Nawrocki, J., Poprawa, P., 2006. Development of Trans-European Suture Zone in Poland: from Ediacaran rifting to Early Palaeozoic accretion. Geol. Q. 50, 59–76.
Orejana, D., Martinez, E.M., Villaseca, C., Andersen, T., 2015. Ediacaran–Cambrian paleogeography and geodynamic setting of the Central Iberian Zone: constraints from coupled U–Pb–Hf isotopes of detrital zircons. Precambrian Res. 261, 234–251.
Paterson, S.R., Ducea, M.N., 2015. Arc magmatic tempos: gathering the evidence. Elements 11, 91–97.
Pearce, J.A., Harris, N.B.W., Tindle, A.G., 1984. Trace-element discrimination diagrams for the Tectonic interpretation of granitic-rocks. J. Petrol. 25, 956–983.
Pereira, M.F., Linnemann, U., Hofmann, M., Chichorro, M., Sola, A.R., Medina, J., Silva, J.B., 2012. The provenance of Late Ediacaran and Early Ordovician siliciclastic rocks in the Southwest Central Iberian Zone: constraints from detrital zircon data on northern Gondwana margin evolution during the late Neoproterozoic. Precambrian Res. 192 (95), 166–189.
Profeta, L., Ducea, M.N., Chapman, J.B., Paterson, S.R., Gonzales, S.M.H., Kirsch, M., Petrescu, L., DeCelles, P.G., 2015. Quantifying crustal thickness over time in magmatic arcs. Sci. Rep. 5.
Shaw, J., Johnston, S.T., 2016. Terrane wrecks (coupled oroclines) and paleomagnetic inclination anomalies. Earth-Sci. Rev. 154, 191–209.
Stampfli, G., Marcoux, J., Baud, A., 1991. Tethyan margins in space and time. Palaeogeogr. Palaeoclimatol. Palaeoecol. 87, 373–409.
Stern, R.J., Ali, K.A., Ren, M., Jarrar, G.H., Romer, R.L., Leybourne, M.I., Whitehouse, M.J., Ibrahim, K.M., 2016. Cadomian (~560 Ma) crust buried beneath the northern Arabian Peninsula: mineral, chemical, geochronological, and isotopic constraints from NE Jordan xenoliths. Earth Planet. Sci. Lett. 436, 31–42.
Stern, R.J., Johnson, P., 2010. Continental lithosphere of the Arabian Plate: a geologic, petrologic, and geophysical synthesis. Earth-Sci. Rev. 101, 29–67.
Streckeisen, A., 1979. Classification and nomenclature of volcanic-rocks, Lamprophyres, Carbonatites, and Melilitic Rocks – recommendations and suggestions of the Iugs Sub-Commission on the systematics of Igneous Rocks. Geology 7, 331–335.
Taylor, S.R., Mclennan, S.M., 1995. The geochemical evolution of the continental-Crust. Rev. Geophys. 33, 241–265.
Thomas, R.J., Ellison, R.A., Goodenough, K.M., Roberts, N.M.W., Allen, P.A., 2015. Salt domes of the UAE and Oman: probing eastern Arabia. Precambrian Res. 256, 1–16.
Ustaomer, P.A., Ustaomer, T., Collins, A.S., Robertson, A.H.F., 2009. Cadomian (Ediacaran–Cambrian) arc magmatism in the Bitlis Massif, SE Turkey: magmatism along the developing northern margin of Gondwana. Tectonophysics 473, 99–112.
von Raumer, J.F., Stampfli, G.M., Arenas, R., Martinez, S.S., 2015. Ediacaran to Cambrian oceanic rocks of the Gondwana margin and their tectonic interpretation. Int. J. Earth Sci. 104, 1107–1121.
Wang, M., Li, C., Ming-Xua, C., 2016. Dating of detrital zircons from the Dabure clastic rocks: the discovery of Neoproterozoic strata in southern Qiangtang, Tibet. Int. Geol. Rev. 58.
Zlatkin, O., Avigad, D., Gerdes, A., 2013. Evolution and provenance of Neoproterozoic basement and Lower Paleozoic siliciclastic cover of the Menderes Massif (western Taurides): coupled U–Pb–Hf zircon isotope geochemistry. Gondwana Res. 23, 682–700.
Zlatkin, O., Avigad, D., Gerdes, A., 2014. Peri-Amazonian provenance of the Proto-Pelagonian basement (Greece), from zircon U–Pb geochronology and Lu–Hf isotopic geochemistry. Lithos 184, 379–392.